Nonlinear Hyperbolic Systems of Generalized Navier-Stokes Type for Interactive Motion in Biology

Wolfgang Alt

Abteilung Theoretische Biologie, Botanisches Institut, Universität Bonn, D-53105 Germany

Summary. We review two modelling approaches to obtain genuinely nonlinear systems of one hyperbolic transport equation (for density) accompanied by parabolic or elliptic equations (for mean velocity and, eventually, pressure), namely generalized Navier-Stokes or (pseudo-stationary) Stokes equations. Background and applications are related to models of interactive biological motion, namely for contractile polymer networks in intra-cellular motility, for cell movement and tissue formation during wound healing as well as for cohorts of migrating birds.

One approach is to derive, after suitable scaling, a formal continuum limit of (stochastic) Hamiltonian equations for 'visco-elastic' multi-particle networks with specific interaction laws. The other consists in the derivation of (highly) viscous two-phase flow equations by minimization of a corresponding energy-loss functional. In both procedures there remain convergence or existence problems to be solved analytically. Some results and a few numerical simulations are shown, particularly for the 1-dimensional case. For further results, technical details and for comparison with other methods we give corresponding references.

1 'Visco-Elastic' Multi-particle Networks in Biological Systems

1.1 Model Setup

Let us describe the Hamiltonian dynamics of N 'particles' constituting a deformable network in $\mathfrak{R}^m$(meant are biochemical or biological entities as 'polymers', 'cells' or 'birds') by standard (stochastic) evolution equations for *positions* $X_i(t) \, \epsilon \, \mathfrak{R}^m$ and *velocities* $V_i(t) \, \epsilon \, \mathfrak{R}^m$, $i = 1, ..., N$:

$$dX_i = V_i \cdot dt \tag{1}$$

$$dV_i = (A_i + \sum_{j \neq i} A_{ij}) \cdot dt + \widetilde{\beta}_i \cdot d\zeta \tag{2}$$

where A_i resp. A_{ij} denote the deterministic acceleration vectors for the i-th 'particle', either induced by its own activity or by interaction with other 'particles', respectively, and where $\widetilde{\beta}_i$ measures the amplitude of small stochastic perturbations, e.g. due to 'thermodynamics' or individual arbitrariness, represented as mutually independent Brownian increments $d\zeta \, \epsilon \, \mathfrak{R}^m$ during infinitesimally small time steps dt.

The first deterministic *acceleration* term in equation (2) might describe a self-induced adjustment to a given *preferred speed* S^*, common for all 'particles', say

$$A_i = \Phi(V_i) = \gamma(\parallel V_i \parallel) \cdot (S^* / \parallel V_i \parallel - 1) \cdot V_i(t). \tag{3}$$

with an *adjustment rate* $\gamma = \gamma(S_i)$ that could depend on the 'particle's actual speed $S_i = \| V_i \|$. In case of $S^* = 0$, the vector $A_i = -\gamma \cdot V_i$ could just describe physical friction force divided by mass. Analogously, the acceleration term A_{ij} could describe the physical interaction force, which the j-th 'particle' exerts onto the i-th one, divided by its body mass. However, for polymer networks, and even more for biological entities like cells or birds, which physiologically respond to interactions with neighbors and then adjust their moving velocity in an active manner, a simple linear superposition in $\sum_{j \neq i} A_{ij}$ is questionable. Therefore, later we will allow the term A_{ij} to depend not only on the variables of the $i \div j$ pair alone. Clearly, in more elaborate models, interaction could be indirectly transmitted by the dynamics of an 'external field' in-between the network particles (see e.g. [7]).

Here we would like to present a model class that considers **nearest neighbor interactions** only. To achieve this in a standard way, we use the well-known **Voronoi tesselation** and complementary **Delaunay triangulation**. For each network node $X_i(t)$ an open *Voronoi neighborhood* $\mathfrak{V}_i(t)$ is defined, the so-called *Voronoi polyeder*, whose boundary $\partial\mathfrak{V}_i(t) = \bigcup_{j \epsilon N_i} \overline{\Delta_{ij}(t)}$ is the concatenation of open $(m-1)$-dimensional *contact surfaces* (or *Voronoi surfaces*)

$$\Delta_{ij}(t) := \{x \epsilon \mathfrak{R}^m : |x - X_i(t)| = |x - X_j(t)| < |x - X_k(t)| \, \forall k \neq i, j\} \neq \emptyset$$

of all thereby defined *nearest neighbors of* i, namely $j \epsilon N_i$. This contact surface Δ_{ij} orthogonally cuts the connecting vector $R_{ij} := X_j - X_i$ exactly at half the *neighbor distance* $r_{ij} := |R_{ij}|$, while the outer surface normal vector is $\nu_{ij} := R_{ij}/r_{ij}$ and the surface content is given by $|\Delta_{ij}| = \tau_{ij} \left(\frac{r_{ij}}{2}\right)^{m-1}$, where τ_{ij} is a measure for the *'space angle'*, under which the i-th 'particle' gets in contact with its j-neighbor. For example, in the 2-dimensional case this angle is $\psi_{ij} = \psi_{ij}^+ + \psi_{ij}^-$, looking to the left and to the right, with $\tau_{ij} = |\tan \psi_{ij}^+ + \tan \psi_{ij}^-|$, see Fig. 1. Obviously, $\bigcup_{i=1}^N \overline{\mathfrak{V}_i(t)}$ constitutes the Voronoi tesselation around the network 'particles'. Dual to this is the Delaunay triangulation of the network hull $\mathfrak{D}(t) = \bigcup_{k=1}^K \overline{\mathfrak{D}_k(t)}$, consisting of all non-empty m-dimensional *Delaunay polyeders* $\overline{\mathfrak{D}_k(t)}$ generated by network nodes $X_i(t)$: If, for instance, $X_i(t) \epsilon \overline{\mathfrak{D}_k(t)}$ is one of its corner points, then the edges emanating from this point are the adjacent connecting vectors R_{ij} to all those nearest neighbors j, whose Voronoi surfaces $\overline{\Delta_{ij}(t)}$ have a non-void mutual intersection; for this constellation we will write $i, j \epsilon N_k^{\mathfrak{D}}$ and $k \epsilon K_{ij}^{\mathfrak{D}}$. Thus, $|\mathfrak{D}_k(t)|$ measures part of the *'free space' volume* between these neighboring network 'particles', see Definition 1.1 below.

We introduce a proper scaling procedure, particularly suited for modelling **nearest neighbor interactions,** the only case that we are going to consider here. Let the **macroscopic length scale** $\mathfrak{L}$ be defined as a quantity in the order of the *network diameter*, and let us assume that it stays bounded, $\mathfrak{L} \sim 1$, on a non-dimensional scale. Furthermore, let δ be the **microscopic length scale** denoting the *mean neighbor distance* within the network. Then, for high *number of network particles*, $N \to \infty$, in a bounded network this mean free distance becomes infinitesimally small, $\delta \simeq \mathfrak{L}/N^{\frac{1}{m}} \to 0$, according to the assumption that in m spatial dimensions

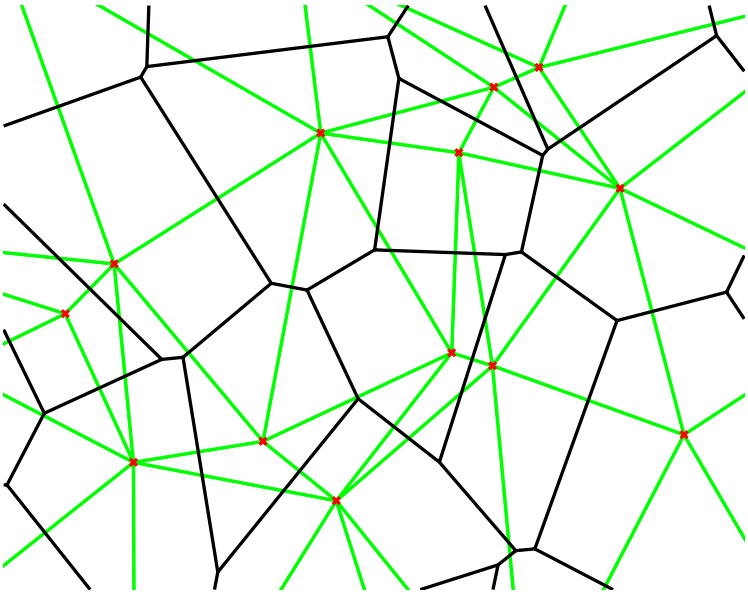

Fig. 1. Part of a 2-dimensional Voronoi-Delaunay triangulation induced by a set of points $X_i(t)$ representing the network of nearest neighbors in a simulated bird swarm; by courtesy from [31]. Obviously, there are regions with lower or higher 'network density ' where accordingly, at least on a local stochastic average, both the Delaunay triangles $\mathfrak{D}_k$ (with grey lines) and the Voronoi polygons $\mathfrak{V}_i$ (black) have larger or smaller size, respectively. Also, nearest neighbor distance r_{ij} and mean size of the two adjacent Delaunay triangles $\mathfrak{D}_k$ with $i, j \,\epsilon\, N_k^{\mathfrak{D}}$ seem to be correlated. Furthermore notice, that the number of neighbors varies between 4 and 7; related statistics for larger swarms and longer runs can be found in [31].

the 'free space' volumes scale as $|\mathfrak{D}_k| \sim \delta^m$ on the average. Then we can introduce two measures of discrete, piecewise constant volume densities on $\mathfrak{D}(t)$, by the following definitions.

Definition 1.1 'Specific Delaunay volume' *function* $E_{\mathfrak{D}}(t,x) := \frac{|\mathfrak{D}_k(t)|}{\delta^m}$ *for* $x \,\epsilon\, \mathfrak{D}_k(t)$, $k = 1, ..., K$,

and its inverse function, namely the

Definition 1.2 ***Delaunay density*** *function* $u_{\mathfrak{D}}(t,x) = \frac{1}{E_{\mathfrak{D}}(t,x)}$,

both being measures '*between' network particles*, and, dual to this,

Definition 1.3 'Specific Voronoi volume' *function* $E_{\mathfrak{V}}(t,x) := \frac{|\mathfrak{V}_i(t)|}{\delta^m}$ *for* $x \,\epsilon\, \mathfrak{V}_i(t) \subset \mathfrak{D}(t)$, *i.e. only for interior network points* $i = 1, ..., N$, *whose Voronoi neighborhood lies in the hull* $\overline{\mathfrak{D}(t)}$,

and its inverse function, namely the

Definition 1.4 ***Voronoi density*** *function* $u_{\mathfrak{V}}(t,x) = \frac{1}{E_{\mathfrak{V}}(t,x)}$,

both being measures *'around' network particles.*

For a typical 2-dimensional example, taken as snapshot from a model simulation run, see Fig. 1. Notice that for a regular network, e.g. a hexagonal one, where each particle has 6 equally distant neighbors, e.g. chosen as an initial configuration for $t = 0$, both density functions would be constant and equal: $u_{\mathfrak{D}}(0,\cdot) = u_{\mathfrak{V}}(0,\cdot)$. Also, for anisotropically deformed but still quite regularly spaced networks, the two densities will have quite similar values, at least on a local stochastic average (as can be observed in Fig. 1). However, depending on the 'particle's dynamics, sometimes they could vary quite much, for instance, in degenerate situations described below; but still the concept of 'density' in the sense of measures can be maintained.

Remark 1.5 *As long as network 'particles' are disjoint, both densities* $u_{\mathfrak{D}}$ *and* $u_{\mathfrak{V}}$ *stay finite step functions, since the Delaunay polyeders do not degenerate (see e.g. [9]). The* i*-th 'particle' cannot cross the boundary of any other polyeder* $\mathfrak{D}_k(t)$ *except at one of its corners; then it collides with another 'particle'* j*. In case of such collisions there appear degenerate polyeders with vanishing volume* $E_{\mathfrak{D}}$*, but still the 'between particle' density* $u_{\mathfrak{D}}$ *is well-defined as* n*-dimensional Hausdorff measure with* $(m-l) \leq n$ *for* l*-fold collisions, such that the subsequent arguments and limit procedures could still be valid in suitably generalized function or measure spaces.*

Generically, i.e. in any cases of non-degenerate collisions, the Voronoi density $u_{\mathfrak{V}}$ *stays bounded. Degeneration would occur, for example in spatial dimensions* $m \geq 2$*, when* $l \geq 2$ *'particles' in a line simultaneously collide.*

For the 1*-dimensional case, with an ordered chain* $X_1(t) < X_2(t) < .... < X_N(t)$*, the 'free space' around the* i*-th interior 'particle' has size* $|\mathfrak{V}_i| = \frac{1}{2}(R_{i(i+1)} + R_{(i-1)i})$*, the mean value of both nearest neighbor distances, with* $|\mathfrak{D}_i| = R_{i(i+1)}$*,* $i = 1, ..., N-1$*. Notice that therefore*

$$u_{\mathfrak{V}}(t,x) = \frac{2\, u_{\mathfrak{D}}(t,x^+)\, u_{\mathfrak{D}}(t,x^-)}{u_{\mathfrak{D}}(t,x^+) + u_{\mathfrak{D}}(t,x^-)}$$

with $x^- = X_i(t)$ *and* $x^+ = X_{i+1}(t)$ *for interval points satisfying* $X_i(t) < x < X_{i+1}(t)$*. Then, if* l *'particles' collide at an interior point* $X_i(t)$*,* $u_{\mathfrak{D}}$ *would there become a Dirac measure proportional to* $(l-1)\delta_{X_i(t)}$*, while* $u_{\mathfrak{V}}$ *would stay bounded for* $l = 2$ *and proportional to* $(l-2)\delta_{X_i(t)}$ *only for* $l \geq 3$*.*

Finally, we construct the following linear interpolations on $\overline{\mathfrak{D}(t)}$

Definition 1.6 ***(Delaunay velocity)*** Piecewise linearly interpolation $\mathbf{v}(t,x)$ *with* $\mathbf{v}(t, X_i(t)) = V_i(t)$ *, for* $i = 1, ..., N$*, i.e.* $\mathbf{v}$ *denotes the* 1*-st order spline interpolation of the velocity vector, by which the Delaunay 'triangulation' of the network is deformed with time,*

and

Definition 1.7 ***(Interpolated Delaunay characteristics)*** *For each point $y \in \overline{\mathfrak{D}(0)}$, the initial network hull, we define the* characteristics $x_y(t)$ *to satisfy*

$$\begin{aligned} \dot{x}_y(t) &= \mathbf{v}\left(t, x_y(t)\right) , \\ x_y(0) &= y . \end{aligned} \tag{4}$$

Since $\mathbf{v}(t,\cdot)$ is piecewise linear, for any $y \in \mathfrak{D}_k(0)$ the characteristics $x_y(t)$ are corresponding linear interpolations of the 'particle's trajectories $X_i(t)$ with $i \in N_k^{\mathfrak{D}}$. Notice, that this definition even holds for stochastic swarm processes (i.e. equation (4) can be written as a stochastic differential equation and thereby establishing stochastic characteristics), provided that products of $V_i(t)$ with $X_i(t)$ are well-defined.

Let us, for any (sufficiently differentiable) function $h(t,\cdot)$ on $\overline{\mathfrak{D}(t)}$, denote the *derivative along characteristics* as

$$d_t h(t,x) \ := \frac{d}{dt} h\left(t, x_y(t)\right), \text{ with } x = x_y(t) \tag{5}$$

$$= \partial_t h(t,x) + \mathbf{v}\left(t,x\right) \cdot \nabla_x h(t,x) \tag{6}$$

then even for the piecewise constant volume and density functions introduced above, the derivative (5) is well-defined and, by using (1) and Gauss' integration law, we can easily derive

Proposition 1.8 ***(Delaunay equations)*** *The 'discrete' volume and density functions 'between particles' defined in Definitions 1.1 and 1.2 satisfy (for any non-zero scaling parameter $\delta > 0$) the following standard constitutive 'volume' or 'mass balance' continuity equations on each $\mathfrak{D}_k(t)$, for $k = 1, ..., K$, thus in a generalized sense on the whole network hull $\overline{\mathfrak{D}(t)}$:*

$$d_t E_{\mathfrak{D}} = E_{\mathfrak{D}} \, \nabla_x \cdot \mathbf{v} , \tag{7}$$

$$d_t u_{\mathfrak{D}} = -u_{\mathfrak{D}} \, \nabla_x \cdot \mathbf{v} . \tag{8}$$

Furthermore, since for the edge vectors $R_{ij} = X_j - X_i$, $i, j \in N_k^{\mathfrak{D}}$, the ordinary differential equation holds

$$\frac{dR_{ij}}{dt} = V_j - V_i = |R_{ij}| \, \frac{V_j - V_i}{|X_j - X_i|} = R_{ij} \ \cdot \nabla_x \mathbf{v} , \tag{9}$$

then at any point $x \in \mathfrak{D}_k(t)$ every small 'tangential' vector $R_x = \widetilde{x} - x \in \mathfrak{R}^m$ can be written by a fixed linear combination of the edge vectors, and we derive for its evolutionary 'transport' along characteristics

$$d_t R_x = R_x \cdot \nabla_x \mathbf{v} . \tag{10}$$

Similarly, Gauss' integration law applied to the Voronoi neigborhoods $\mathfrak{V}_i(t)$ yields analogous continuity equations, though with a more refined interpolation of the velocities $V_i(t)$:

Proposition 1.9 ***(Voronoi equations)*** *The 'discrete' volume and density functions 'around particles' defined in Definitions 1.3 and 1.4 satisfy (for any non-zero scaling parameter $\delta > 0$) the following standard constitutive 'volume' or 'mass balance' continuity equations on each $\mathfrak{V}_i(t) \subset \mathfrak{D}(t)$, therefore in a generalized sense on the whole 'interior' network domain $\overline{\mathfrak{D}_{\mathfrak{V}}(t)} := \bigcup_{i \in \check{N}} \overline{\mathfrak{V}_i(t)}$*

$$d_t E_{\mathfrak{V}} = E_{\mathfrak{V}} \, \nabla_x \cdot \widetilde{\mathbf{v}} \,, \tag{11}$$

$$d_t u_{\mathfrak{V}} = -u_{\mathfrak{V}} \, \nabla_x \cdot \widetilde{\mathbf{v}} \,, \tag{12}$$

where we use the following

Definition 1.10 ***(Voronoi velocity)*** Piecewise linear 'refined' interpolation $\widetilde{\mathbf{v}}(t,x)$ *with $\widetilde{\mathbf{v}}(t, X_i(t)) = V_i(t) = \mathbf{v}(t, X_i(t))$ for $i = 1, ..., N$, as in Definition 1.6 but with the additional requirement $\widetilde{\mathbf{v}}(t, Z_l(t)) = \dot{Z}_l(t)$ for every corner point $Z_l(t)$ of any Voronoi polyeder $\partial\mathfrak{V}_i(t)$, i.e. $\widetilde{\mathbf{v}}$ denotes the velocity, by which the Voronoi tesselation of the network is deformed with time.*

By elementary calculations one can easily prove, at least in the 2-dimensional case, the

Proposition 1.11 ***(Relation between Delaunay and Voronoi velocities, explicitly given for $\mathbf{m = 2}$)***

For any triple $i, j, k \in N_l^{\mathfrak{D}}$, whose positions define the corners of a Delaunay triangle $\mathfrak{D}_l(t)$, its geometric center $z = Z_l(t)$ with equal distance $|z - X_\iota(t)|$ for all $\iota \in N_l^{\mathfrak{D}}$, thus representing a potential boundary node $\{z\} = \Delta_{ij} \cap \Delta_{ik}$ of the Voronoi polyeder $\mathfrak{V}_i(t)$, moves according to the following differential equation, linear in the Delaunay velocities

$$\dot{Z}_l(t) = \widetilde{\mathfrak{P}}_{\mathfrak{D}_l}[V_i, V_j, V_k] = V_i + \frac{1}{2}\mathfrak{P}_{R_{ij}^{\perp}}(V_k - V_i) + \frac{1}{2}\mathfrak{P}_{R_{ik}^{\perp}}(V_j - V_i)$$

where $\mathfrak{P}_{R_{ij}^{\perp}}$ denotes the orthogonal projection onto the line $R_{ij}^{\perp}$ orthogonal to a boundary edge vector R_{ij}.

Notice that the center point $Z_l(t)$ can move outside the triangle $\mathfrak{D}_l(t)$, depending on how flat this is. Several such cases can be seen in Fig. 1, however, the center point always stays relatively near to the triangle's boundaries.

Thus generally, also for higher space dimensions, an estimation how far the Voronoi velocity $\widetilde{\mathbf{v}} = \dot{Z}_l(t)$ deviates from the Delaunay velocity $\mathbf{v}$ depends on the degree of degeneracy of the Delaunay polyeders in the network. Therefore, in the following we suppose a non-degeneracy condition which would guarantee that the Voronoi velocity $\widetilde{\mathbf{v}} = \widetilde{\mathfrak{P}}_{\mathfrak{D}_l}[\mathbf{v}]$ is *subordinate* to $\mathbf{v}$ in the sense of a uniform estimate $|\widetilde{\mathbf{v}}| = O(|\mathbf{v}|)$ i.e. boundedness of the linear operator $\widetilde{\mathfrak{P}}_{\mathfrak{D}_l}$ for each Delaunay polyeder $\mathfrak{D}_l$. Let us call this the **Delaunay uniformity criterium**.

Finally, in order to reformulate the dV_i model equations (2) in terms of the density and velocity interpolations defined above (Definitions 1.1–1.4) we assume a special rescaled **model for mutual acceleration**, namely

$$A_{ij} = \frac{|\Delta_{ij}|}{\delta^m |R_{ij}|} \cdot \left[\widetilde{\alpha}_{ij} \, R_{ij} + \widetilde{\mu}_{ij} \, \frac{dR_{ij}}{dt} \right] \text{, for } i,j = 1, ..., N \tag{13}$$

reminding that $|\Delta_{ij}| = \tau_{ij} \left(|R_{ij}| / 2 \right)^{m-1}$. Thus, up to the first factor, the interaction between the i-th and the j-th 'particle' is supposed to depend linearly on the 'sensed' mutual distance R_{ij} and its temporal derivative $\frac{dR_{ij}}{dt}$, which is a reasonable, though the simplest assumption for biologically interactive entities. However, the coefficients $\widetilde{\alpha}_{ij}(t)$ and $\widetilde{\mu}_{ij}(t)$ will depend on other interactive conditions, in particular other nearby neighbors, see the discussion below. In any case, let us think of them as constant functions on any Voronoi contact surface $\Delta_{ij}(t)$. Moreover, notice that the factor in front of the brackets in (13) provides a weight term inversely proportional to neighbor distance $|R_{ij}|$ and proportional to $|\Delta_{ij}(t)|$, the latter measuring the degree of contact between the two neighbors. Both model assumptions are very reasonable, because thereby a newly appearing nearest neighbor j will first have a vanishingly small influence that will increase, the more it enters the 'interaction scope' of the i-th 'particle' being quantified by $\tau_{ij} = (2/|R_{ij}|)^{m-1} |\Delta_{ij}(t)|$. Thus, using (9) and observing that $R_{ij} \cdot \nabla_x \mathbf{v}$ is the same constant vector on each $\mathfrak{D}_k(t)$ with $k \, \epsilon \, K_{ij}^{\mathfrak{D}}$, we can write the sum in the second term of equation (2) as a boundary integral over the Voronoi polyeders $\partial \mathfrak{V}_i = \bigcup_{j \epsilon N_i} \overline{\Delta_{ij}}$ with outer normal vector $\nu = \nu_{ij} = R_{ij} / |R_{ij}|$ on each boundary surface Δ_{ij}, and then use Gauss' law to obtain a divergence term:

$$\sum_{j \neq i} A_{ij} = \frac{1}{\delta^m} \sum_{j \epsilon N_i} |\Delta_{ij}| \, \nu_{ij} \cdot [\widetilde{\alpha}_{ij} \, \mathbf{I} + \widetilde{\mu}_{ij} \, \nabla_x \mathbf{v}] \tag{14}$$

$$= \frac{1}{\delta^m} \int\limits_{\partial \mathfrak{V}_i} \nu \cdot [\widetilde{\alpha}_{ij} \, \mathbf{I} + \widetilde{\mu}_{ij} \, \nabla_x \mathbf{v}] \tag{15}$$

$$= \frac{1}{\delta^m} \int\limits_{\mathfrak{V}_i} \nabla_x \cdot [\widetilde{\alpha}_{ij} \, \mathbf{I} + \widetilde{\mu}_{ij} \, \nabla_x \mathbf{v}] \tag{16}$$

$$= \frac{1}{u_{\mathfrak{V}}} \nabla_x \cdot [\widetilde{\alpha}_{ij} \, \mathbf{I} + \widetilde{\mu}_{ij} \, \nabla_x \mathbf{v}] + O(\delta) \tag{17}$$

where equality (16) with derivatives and integration only holds in a weak (distributional) sense and where the smallness of the error term in (17) would strongly depend on the kind of convergence in the continuum limit $\delta \to 0$, see part of the following discussion.

Modelling assumptions. Before we turn to this important point, let us discuss the modelling coefficients $\widetilde{\alpha}_{ij}$ and $\widetilde{\mu}_{ij}$ in formula (13) above. If the network 'particles' would just be physically connected by elastic springs with a common equilibrium elongation r_*, then we would have $\widetilde{\alpha}_{ij} \simeq \widehat{\alpha}(r_{ij}) (r_{ij} - r_*)$ with some $\widehat{\alpha} > 0$, meaning repulsion for $r_{ij} < r_*$ and attraction for $r_{ij} > r_*$. However, biological entities, or even biopolymers, can develop much more complex interactions in a connected network. For instance, in space dimensions $m \geq 2$, repulsion or attraction could depend on the *'free interaction volume'* in the space around the connecting vector R_{ij}, e.g. expressed as a mean value of all adjacent Delaunay polyeder volumes $|\mathfrak{D}_k|$, namely

$\widetilde{\alpha}_{ij} = \widetilde{\alpha}_{ij}\left(|\mathfrak{D}_k|,\ k\,\epsilon\, K_{ij}^{\mathfrak{D}}\right) = \alpha\left(\delta^m \left|K_{ij}^{\mathfrak{D}}\right| / \sum_{k\,\epsilon\, K_{ij}^{\mathfrak{D}}} |\mathfrak{D}_k|\right)$, where $\alpha(u)$ would denote a monotone decreasing function of an averaged Delaunay density, $u = \overline{u_{\mathfrak{D}}}^{ij}$, positive (i.e. attracting) for low densities u, and negative (i.e. repulsing) for higher densities, with an equilibrium density u_*. For instance, in the 2-dimensional case

$$\overline{u_{\mathfrak{D}}}^{ij} = \frac{2\, {u_{\mathfrak{D}}}^{k+}\, {u_{\mathfrak{D}}}^{k-}}{{u_{\mathfrak{D}}}^{k+} + {u_{\mathfrak{D}}}^{k-}}$$

is a generalized mean between the Delaunay densities ${u_{\mathfrak{D}}}^k := u_{\mathfrak{D}}|_{\mathfrak{D}_k}$ regarding the two joining neigbors $k_+, k_- \in K_{ij}^{\mathfrak{D}}$. Similarly, we could assume that the 'viscosity' coefficients $\widetilde{\mu}_{ij}$ also depend on the surrounding 'free interaction volume', $\widetilde{\mu}_{ij} = \mu\left(\delta^m \left|K_{ij}^{\mathfrak{D}}\right| / \sum_{k\,\epsilon\, K_{ij}^{\mathfrak{D}}} |\mathfrak{D}_k|\right)$, now with $\mu(u) > 0$ and eventually increasing for higher densities $u = \overline{u_{\mathfrak{D}}}^{ij}$.

1.2 Continuum Limit

Assuming that in the continuum limit, $\delta \to 0$, the above defined Delaunay and Voronoi density functions (or measures) $u_{\mathfrak{D}}$ and $u_{\mathfrak{V}}$ as well as the Delaunay and Voronoi velocities $\mathbf{v}$ and $\widetilde{\mathbf{v}}$ converge, in a suitably defined stochastic sense (e.g. in some configuration space [25]) and form a limit network domain $\mathfrak{D}(t) = \text{supp}[\, u_{\mathfrak{D}}(t.\cdot)]$, then we could formulate the following

Conjecture 2. In a formal limit as $\delta \to 0$, the density measures and velocity functions defined above, as realizations of a suitably scaled and averaged stochastic limit process, fulfill the **stochastic Lagrange equations of Navier Stokes type** along stochastic characteristics as in Def. 6

$$d_t u_{\mathfrak{D}} = -u_{\mathfrak{D}}\, \nabla_x \cdot \mathbf{v}\,, \tag{18}$$

$$d_t u_{\mathfrak{V}} = -u_{\mathfrak{V}}\, \nabla_x \cdot \widetilde{\mathbf{v}}\,, \tag{19}$$

$$d_t \mathbf{v} = \Phi(\mathbf{v}) + \frac{1}{u_{\mathfrak{V}}} \nabla_x \cdot [\alpha(u_{\mathfrak{D}})\, \mathbf{I} + \mu(u_{\mathfrak{D}})\, \nabla_x \mathbf{v}] + \beta\, \Xi. \tag{20}$$

Here the properties of the additive stochastic term Ξ (e.g. the standard $(m+1)$-dimensional white noise of the so-called Brownian sheet process) and expressions for its amplitude, β, would depend on corresponding stochastic convergence theorems that still have to be proven. In the simple 1-dimensional case first results in this direction have been obtained in [6]:

Remark 1.12 ***(Results for space dimension*** $m = 1$***)*** *For an ordered* 1*-dimensional chain (as in Remark 1.5) the model assumptions in Section 1.1 above would be consistent with nearest neighbor distance dependent coefficients* $\widetilde{\alpha}_{ij} = \alpha\left(\frac{\delta}{r_{ij}}\right)$ *and* $\widetilde{\mu}_{ij} = \mu\left(\frac{\delta}{r_{ij}}\right)$*. Under suitable conditions on the behavior of* $\Phi(\mathbf{v})$*,* $\alpha(u)$ *and* $\mu(u)$*, as well as for suitable scaling of the stochastic amplitude, namely* $\widetilde{\beta}_i \sim \sqrt{\delta}$ *in model*

equations (1–2), certain transformations and estimations can be performed yielding the continuum limit equations (18–20) above, with $u_{\mathfrak{V}} = u_{\mathfrak{D}} = u$, $\mathbf{v} = \widetilde{\mathbf{v}}$, *the stochastic term* $\Xi = \Xi_{t,x}$ *representing independent infinitesimal increments of the standard temporal-spatial Brownian sheet and the stochastic amplitude scaling as* $\beta \sim \sqrt{u}$, *for details see [6].*

Convergence Assumption: Generally, let us assume that the initial network configuration, at $t = 0$, had been chosen so that in the limit $\delta \to 0$ the two densities coincide, $u_{\mathfrak{V}}(0, \dot{)} = u_{\mathfrak{D}}(0.\dot{)}$. Moreover, let us suppose that the stochastic network fulfills a **uniformity criterium** (as defined in section 1.1) such that the more refined Voronoi velocity $\widetilde{\mathbf{v}} = \widetilde{\mathfrak{P}}_{\mathfrak{D}_l}[\mathbf{v}]$, by inducing relatively fast oscillations of the geometric centers $Z_l(t)$ around the Delaunay polyeders $\mathfrak{D}_l(t)$, after local averaging (on a relatively fast time scale) converges to the same limit as the Delaunay velocity $\mathbf{v}$; thus we would have $\widetilde{\mathbf{v}} = \mathbf{v}$ for $\delta \to 0$, as it holds for the 1-dimensional case. Clearly, then equations (18,19) would also imply the asymptotic equality $u_{\mathfrak{V}} = u_{\mathfrak{D}} =: u$.

Furthermore, let us suppose that, for a certain time interval, these convergences are valid in suitable function or measure spaces including the stochastics (e.g. again in some configuration space, cf. [25]). Then, by computing the derivative along characteristics (6), i.e. by performing the standard transformation from Lagrangian into Euler coordinates, we can formulate the

Conjecture 3. Under the *convergence assumptions* stated above, the stochastic differential equation system (18–20) would in the formal limit $\delta \to 0$ lead to the following **stochastic Navier-Stokes equations** for u and $\mathbf{v}$:

Hyperbolic continuity equation (mass balance)

$$\partial_t u + \nabla_x \cdot (u\mathbf{v}) = 0 \tag{21}$$

Stochastic parabolic velocity equation (impulse balance)

$$\partial_t \mathbf{v} + \mathbf{v} \cdot \partial_x \mathbf{v} = \Phi(\mathbf{v}) + \frac{1}{u} \nabla_x \cdot [\alpha(u)\, \mathbf{I} + \mu(u)\, \nabla_x \mathbf{v}] + \beta(u)\, \Xi. \tag{22}$$

If, in contrast to the modelling assumptions above, for dimensions $m \geq 2$ the 'elasticity' and 'viscosity' coefficients $\widetilde{\alpha}_{ij}$ and $\widetilde{\mu}_{ij}$ explicitely depend on nearest neighbor distance r_{ij} or, in general, on some other derived quantities of the network configuration, then there are two possibilities to proceed:

Remark 1.13 *(a) In case the stochastic perturbations are strong enough, so that the network configuration is isotropically mixed on macroscopic time scales, then similar ideas as in mean field approximations (still to be worked out in this situation) could be used to argue that the mean distance 'between particles' satisfies an asymptotic relation*

$$\frac{r}{\delta} = (u_{\mathfrak{D}})^{\frac{1}{m}} \text{ for } \delta \to 0.$$

Then we would again obtain a but modified functional dependence $\alpha = \alpha(u)$ *and* $\mu = \mu(u)$ *in the limit equation (22).*

(b) For small stochastic perturbations and relatively mild elasticity and viscosity coefficients, one might be able to prove the uniformity criterium (defined in section 1.1), such that the linear deformation equation (10) along characteristics holds in the continuum limit and is solvable, at least for a certain time interval. Thus, starting with an initial network deformation tensor, $D_0(y)$*, say isotropic, then for any* $y \in \mathfrak{D}(t)$ *there would exist a generalized semigroup* $U_y(t) \in \mathfrak{R}^{m\times m}$*, with* $d_t U_y(t) = U_y(t) \cdot \nabla_x \mathbf{v}(t, X_y(t))$ *which would yield for each point* $x = X_y(t)$ *at time* t *a deformation tensor* $D(t, x)$*. It describes the anisotropy in the continuum network so that in each direction* $\theta \in \mathfrak{S}^{m-1}$ *the 'rescaled particle distance' in this direction could be computed as* $\widehat{r}_\theta(t, x) = \theta \cdot D(t, x) \cdot \theta^T$*. Also, we would regain the Delaunay density* $u_{\mathfrak{D}}$ *from* $\det D(t, x) = E_{\mathfrak{D}}(t, x) = \frac{\delta^m}{u_{\mathfrak{D}}(t,x)}$*. Details of this procedure, which requires the derivation of constitutive continuum equations for the deformation tensor* $D(t, x)$*, still have to be elaborated.*

1.3 Boundary Conditions

So far, our formal derivation of the differential equation system (21,22) is valid only in the interior of the limit continuum network domain $\mathfrak{D}(t)$. Thus, it can be directly extended to situations, where a 'locally uniform' network spans the whole space $\mathfrak{R}^m$. However, for domains with finite *moving boundary* $\partial\mathfrak{D}(t)$ one has to prove sufficient smoothness and derive certain induced 'natural' boundary conditions. For the 1-dimensional case of a *finite visco-elastic chain* this has been worked out in [6], where 'natural' Neumann boundary conditions for the velocity $\mathbf{v}$ appear, corresponding to a continuum model assumption of 'zero tension' at the two chain ends $x = X_\pm(t)$. Clearly, the second 'natural' boundary condition means, that the chain ends move with boundary velocity, $\dot{X}_\pm(t) = \mathbf{v}(t, X_\pm(t))$.

The standard generalization of this latter boundary condition for spatial dimensions $m > 1$, namely

$$d\Gamma/dt = \nu \cdot \mathbf{v}(t, \cdot)|_\Gamma \tag{23}$$

for the free boundary $\Gamma(t) := \partial\mathfrak{D}(t)$ with outer normal vector ν, would directly follow from the fact that the mass balance equation (21), for suitable definition of $u = 0|_{\mathfrak{R}^m\setminus\mathfrak{D}(t)}$, holds on the whole space $\mathfrak{R}^m$ in a distributional sense. However, the definition of the outer normal ν will strongly depend on a necessary, not at all straight-forward algorithm to define appropriate 'closures' of the discrete network domain $\mathfrak{D}(t)$, see [9, 31] for the 2-dimensional case.

1.4 Examples

Visco-elastic polymer networks. When considering the dynamics of, say 2-dimensional, polymer networks (e.g. thin films of polyacrylamid, used as substrates for experimental cell crawling on top of it), then after transforming the original model system to dimensionless coordinates one realizes that, for time and space scales of interest, all non-dimensional rate parameters in model equations (2,3 and

13) with $S^* = 0$, namely γ, $\widetilde{\alpha}$ and $\widetilde{\mu}$, are relatively large, meaning that friction, elasticity and viscosity forces all dominate inertial forces. Thus (2) might be replaced by an explicit pseudo-steady state equation for the i-th 'particle's velocity, $V_i = \frac{1}{\gamma}\left(\sum_{j\neq i} A_{ij} + F_i\right)$, thereby neglecting stochastic perturbations and assuming an additional outer forces F_i acting on each polymer. In the continuum limit (22) this corresponds to the pseudo-steady elliptic Stokes equation

$$\nabla_x \cdot [\alpha(u)\,\mathbf{I} + \mu(u)\,\nabla_x \mathbf{v}] + F = \gamma u \mathbf{v} \tag{24}$$

with eventual boundary conditions and a given outer force vector field F. Notice that this derived model equation for a highly *visco-elastic medium* consists in a simple force balance equation with viscosity and friction coefficients appearing as usual, but the elasticity being described by an isotropic tension term, for example the simplest linear case $\alpha(u) = \alpha_0\,(u_* - u)$. This clearly means that for densities u higher than the equilibrium density u_* the network elasticity (repulsion between polymers) induces a positive pressure, whereas a positive tension for lower densities, quite plausible phenomenological model assumptions. However, we should emphasize, that our derivation of (24) as a continuum limit of a discrete polymer network model is (formally) valid only with the special *modelling assumptions* proposed at the end of Section 1.1, meaning that elastic and viscous forces between connected polymers have a very special form in dependence of 'free space volume' and nearest neighbor distance, see equations (13). For more general modeling dependences probably one has to rely on additional anisotropic tensor equations as indicated in Remark 1.13(b).

For the linear elasticity parameter function (as above) and for constant viscosity parameter $\mu = \mu_0$, Till Bretschneider [11] has used these equations to simulate the deformations of visco-elastic polymer substrates under the influence of two or more migrating cells, which are distributed over a substratum, apply traction forces onto it and (by responding to the experienced substrate tension) move towards each other. This corresponds to experimental observations, which have been studied in detail [19],[28]. In these papers Micah Dembo even solves the inverse problem of computing the cell traction forces from observed displacements of fluorescent beads embedded into the substratum. For results of numerical simulations (as well as analytic investigations for $m = 1$) we refer to [11] and [7].

Bird swarms. For the 1-dimensional case the stochastic model equations (1–2) well describe the dynamics of ordered chains, which we find in migrating bird as cranes or wild geese. For reasonable choices of the distance dependent parameter functions, i.e. $\widetilde{\alpha} = \alpha(\delta/r)$ and $\widetilde{\mu} = \mu(\delta/r)$, and properly scaled stochastic noise, $\widetilde{\beta}_i \sim \sqrt{\delta}$, see Remark 1.12, numerical simulations reveal characteristic phenomena of so-called condensation waves travelling in both directions with a remarkably constant wave speed, see [6]. It turns out, that for a series of decreasing $\delta \simeq \mathfrak{L}/N \to 0$, say with particle number $N = 30, ..., 150$, for example, these condensation waves remain and carry about the same wave speed, see Fig. 2. Therefore the challenging question was, whether the limiting stochastic Navier-Stokes equations (21–22) with natural free boundary conditions would reproduce the same phenomenon of condensation

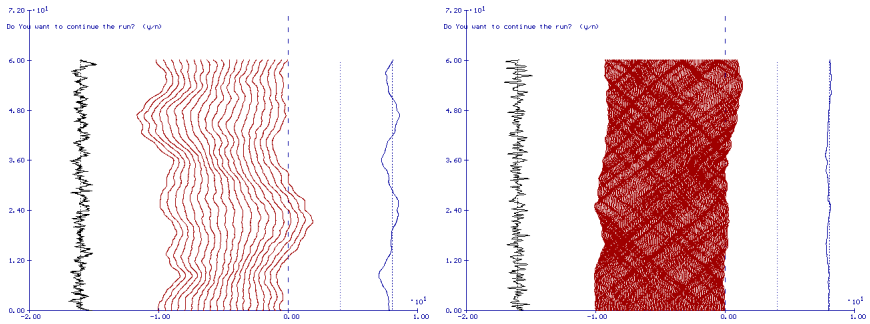

Fig. 2. For a 1-dimensional stochastic bird swarm model with correct scaling of the noise amplitude, $\widetilde{\beta}_i \sim \sqrt{\delta} \sim 1/\sqrt{N}$, the two pictures plot the positions of N birds ($N = 30$ in the left hand picture, $N = 150$ in the right hand one) over time (from 0 to 60 sec, in vertical direction). Here the uniform motion of the migrating birds with positive speed S^* has been substracted. Moreover, to the very left of each picture the fluctuating acceleration is plotted, which the leftmost bird experiences over time, whereas to the very right the fluctuations of the swarm diameter over time can be read off. Both simulations show characteristic condensation waves running through the swarm in both directions with a quite constant speed. From [6].

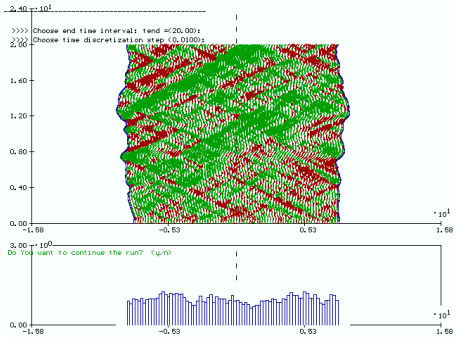

Fig. 3. For the 1-dimensional stochastic Navier-Stokes system arising as continuum limit equations for $\delta \to 0$ from the multi-particle model in Fig. 2, a suitable discretization of the temporally varying swarm interval (divided into $N = 70$ compartments) leads to a typical density distribution (at time $t = 20$), plotted in the lower panel, whereas the upper panel plots the whole density evolution with time (from 0 to 20 sec, in vertical direction). Comparison with the right hand picture in Fig. 2 reveals a striking similarity in the appearance of stochastic waves with constant speed as well as stochastic fluctuations of the two swarm boundaries in both the continuum model and the multi-particle model with $N = 150$ birds. For more details consult [6].

waves. Indeed, a suitable discretization procedure (with appropriate modifications of the Neumann boundary conditions mentioned in Section 1.3 above) produces numerical simulations with quite similar types of stochastically induced waves, see Fig. 3.

Also for higher dimensional cases the stochastic model equations (1–2) have been considered, but so far only with distance dependent 'elasticity' and 'viscosity', see [24] for $m = 3$, and [13, 22, 31] for $m = 2$. Nevertheless, the performed stochastic simulations of 2-dimensional swarms (Figs. 4 and 5) show characteristic behavioral properties resembling 'oscillating clouds' with quite smooth boundaries and quite persistent positional arrangement of 'birds', even in configurations with remarkable variations of swarm shape and internal density distributions. Therefore, it seems to be worth to check whether (with the type of used parameters) these discrete stochastic systems satisfy the *uniformity condition* which was assumed in Section 1.2 above, in order to derive a continuum limit of generalized Navier-Stokes type, although the purely distance dependence of the coefficients (without the 'interaction scope' factor in (13)) creates a difficulty to subsume the hitherto studied models in higher spatial dimensions under the presented model class.

Even independent of such multi-particle models and their analysis, also purely phenomenological continuum models for *cooperative motion* (as in bird swarms or in colonies of gliding bacteria) have been proposed and investigated, which – merely a surprise – again are nonlinear hyperbolic-parabolic or -elliptic systems of Navier-Stokes or Stokes type, respectively, with white noise stochastics, see [12],[13] and [35],[36]. Physical scaling arguments and numerical simulations show characteristic features of phase transitions from a trivial 'disordered' state to 'cooperative' states if, for example, the noise amplitude is successively increased.

However, so far there has been no trial to expand the analysis of such types of continuum models to biologically and mathematically interesting situations with *free boundaries* as in the 1-dimensional case (see Fig. 3).

1.5 Discussion

The here presented construction of 'densities' for dynamic multi-particle systems, the proposed scaling procedure and the subsequent (formal) derivation of a generalized Navier-Stokes system as continuum limit equations (furtheron called the *Voronoi-Delaunay limit*) are, to my knowledge, new and clearly contrast with the usually applied construction and scaling procedure of the so-called *hydrodynamical limit*, cf. [34],[32],[33].

1. **(Densities)** For any open test domain $\mathfrak{U}_\delta \subset \mathfrak{R}^m$ with $|\mathfrak{U}_\delta| \sim \delta^m$ the *hydrodynamical limit* procedure defines a discrete 'particle density' as the sum of Dirac measures $u|_{\mathfrak{U}_\delta} := \sum_{X_i \in \mathfrak{U}_\delta} \delta_{X_i}$ of all particles contained in $\mathfrak{U}_\delta$, thus, as an element in the space $\mathfrak{D}_0$ of distributions on $\mathfrak{R}^m$. Therefore its generic regularity is m degrees lower when compared to the *Voronoi and Delaunay densities* $u_{\mathfrak{V}}$ and $u_{\mathfrak{D}}$ which generically are bounded measurable step functions on $\mathfrak{R}^m$ and

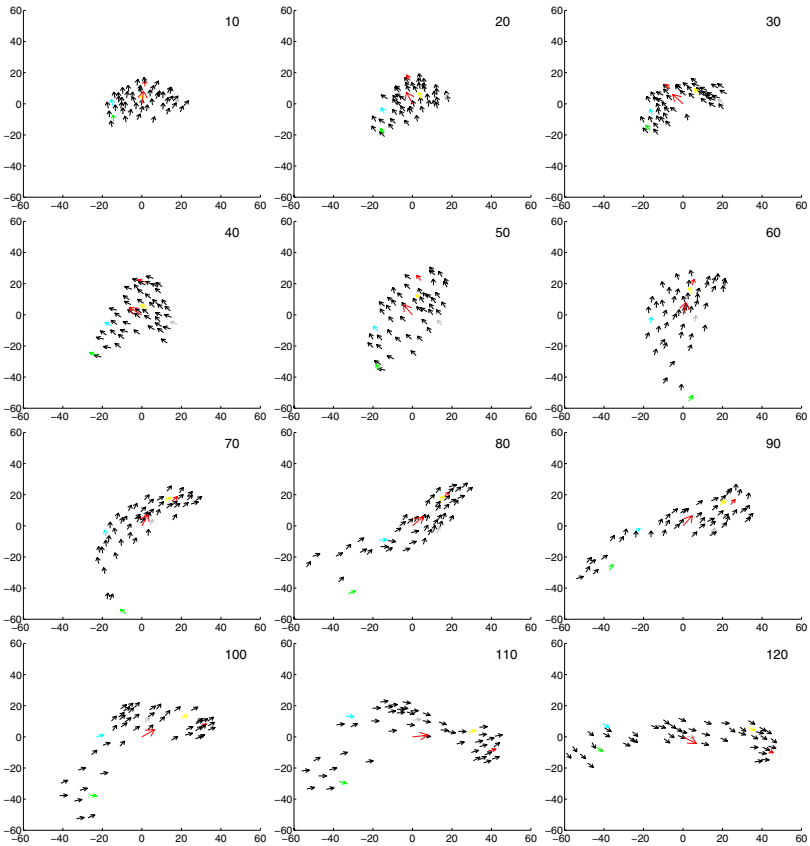

Fig. 4. Simulation of the 2-dimensional bird swarm model with center of mass held fixed and $N = 30$ birds. (12 frames plotted each 10 sec, in 4 lines starting from left). Observe the almost persistent connectivity of the deforming 'network' in spite of extensive elongation of its droplike shape. Also, during its deformation and shearing rotation (i.e. rotation of birds' mean orientation), the relative positions of single birds within the swarm and with respect to each other are, up to small stochastic fluctuations, merely changed (for example, follow the two grey arrows in the very left part of the swarm). From [31] by courtesy of Ralf Müller.

(because of the stochastics only transiently) might degenerate into successively lower dimensional Hausdorff measures, see Remark 1.5.

2. **(Scaling)** In the limit $\delta \to 0$ the *hydrodynamical limit* procedure requires that the test domains $\mathfrak{U}_\delta$, in which e.g. particle collisions are evaluated on the average, still contain (with $N \to \infty$) an infinitely increasing number of particles. Thus, the appropriate scaling has to be chosen as $\delta \simeq \mathfrak{L}/N^\kappa \succ \mathfrak{L}/N^{\frac{1}{m}}$ with an exponent $\kappa > \frac{1}{m}$, contrasting to the generic properties of the *Voronoi-Delaunay limit*, where $\delta \simeq \mathfrak{L}/N^{\frac{1}{m}}$ is chosen as the mean nearest neighbor distance, therefore

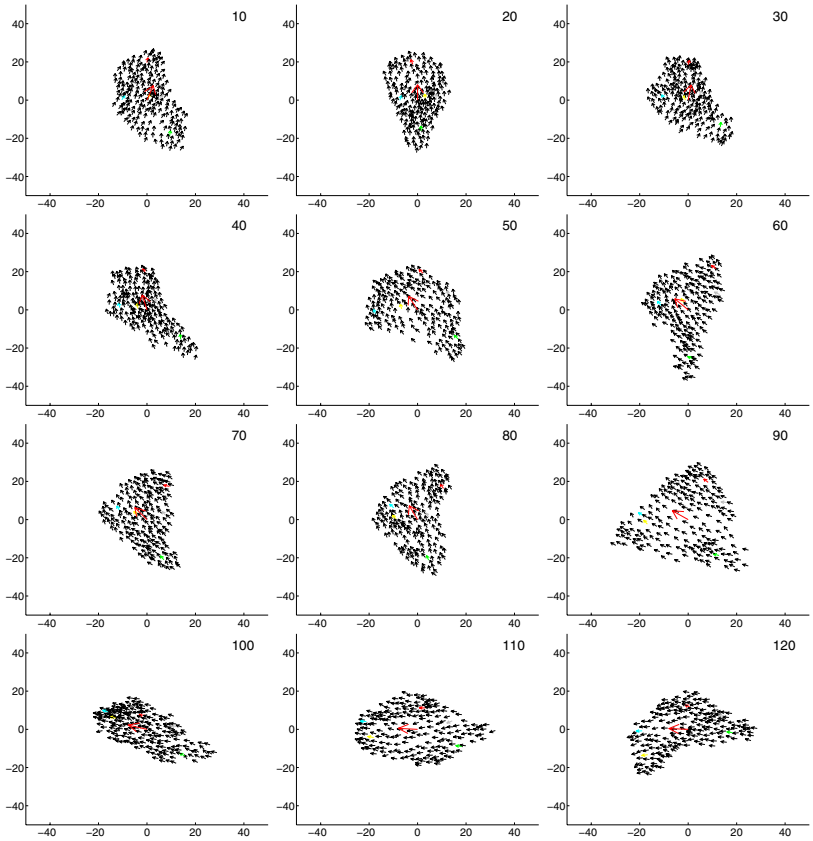

Fig. 5. Analogous plot of model simulations as in Fig. 4, but with $N = 200$ birds and appropriate rescaling of model parameters. Observe here, in addition, the remarkably smooth 'free boundary' of the swarm during extensive shape changes (droplike, triangular, oval), contraction or expansion, and clearly visible transient local accumulations or dilutions, i.e changes in local 'density' (both 'Voronoi' or 'Delaunay' depending on the observer's view, see Definitions 1.1–1.4 in Section 1.1). From [31].

any ball $\mathfrak{U}_\delta := \mathfrak{B}_{C\delta}$ with radius $C\delta$ would generically contain only a uniformly bounded number of 'particles'.

3. **(Stochastics)** As a typical 'mean field approximation' of a stochastic multi-particle process the *hydrodynamical limit* supposes that, at a time scale which is short relative to modelling time, positions of particles are well-mixed, so that averaging can be performed. In contrast, the *Voronoi-Delaunay limit* has to suppose some kind of 'uniformity criterium' (as assumed in Section 1.2); this allows such deformations of the multi-particle network that, at least for an 'interior particle', relative position and identity of its nearest neighbors may change, but the overall shape of its Voronoi neighborhood as well as the number of nearest neighbors (generically identical to the number of corner points of the

Voronoi polyeder) varies only within certain limits. For the 2-dimensional case compare Fig. 1 as well as the simulations in Figs. 4 and 5.

Thus, the required convergence estimates which still have to be performed in order to conclude a rigorous validity of the formally derived *Voronoi-Delaunay limit* equations, would rely on proving sufficient regularity even of higher derivatives of the velocity (e.g. the deformation tensor), similar to but probably more intricate as in the simpler 1-dimensional case. Such estimates could even be generalized to modelling situations, in which the limiting equations are not of simple Navier-Stokes type, see Remark 1.13. Moreover, let me emphasize that already in the simpler case of the *diffusion limit*, stochastic convergence of a discrete particle process to a Brownian sheet is quite easy to be proven in the 1-dimensional case, but more difficult in higher space dimension, see e.g. [25].

In spite of these remaining mathematical problems in analysis and stochastics, the presented technique of Delaunay triangulation and Voronoi tesselation for multi-particle systems has, in the mean time, been used by several authors for modelling and simulating cooperative motion of biopolymers in cells and of cells in tissues, see [9],[10],[30] and the review article [20]. On the other hand, simulations of discretized continuum models of Navier-Stokes types have been studied, e.g. in [12]. The ideas presented here, namely to formulate an appropriate framework for using the *Voronoi-Delaunay limit*, might stimulate further efforts to bring both modelling approaches into closer contact, with the aim to better understand the essential dynamics of interacting biological entities, see also [7].

2 Two-Phase Flow Models for Intracellular Polymer Dynamics

The following derivation is valid for general two-phase composite materials, where a *complex polymer phase*, e.g. in applications to biological cell motility the so-called '*cytoskeleton'* (more or less cross-linked filaments of actin polymers), is embedded within a more fluid material, subsequently called the *aqueous phase* (mainly the 'solvent' in a cell containing all kinds of monomers and polymer fragments). Both phases will be regarded as connected, cohesive and fluid-like. By the latter requirement we simply mean that the interconnections within a given phase are not permanent as in an elastic solid but rather are breaking and rearranging so that over some time scale elastic stresses are eventually relaxed.

For the essential continuum variables, scalar or vector functions of space $\mathbf{x}$ and time t, we use a simplifying notation:

– volume fraction of the *complex polymer phase*: $\theta_c = \theta$ with mean velocity $\mathbf{v}$
– volume fraction of the *aqueous phase*: $\theta_a = (1 - \theta_c)$ with mean velocity $\mathbf{w}$

2.1 Mass Balances

The first mass balance holds for the *volume fraction of the complex polymer phase*, θ_c and is expressed as a hyperbolic equation

$$\partial_t \theta_c + \nabla \cdot (\theta_c \mathbf{v}) = R_c(\theta_c, \theta_a) \; . \tag{25}$$

Here the source term R_c denotes the rate of chemical production of cytoskeletal (e.g. actin filaments) per unit volume. Obviously, there is a corresponding loss of mass from the solvent phase since small precursors of the filament system are regarded as being part of the aqueous phase (e.g. actin monomers). This yields a corresponding second mass balance equation for the *volume fraction θ_a of the aqueous phase*

$$\partial_t \theta_a + \nabla \cdot (\theta_a \mathbf{w}) = R_a(\theta_c, \theta_a) \; . \tag{26}$$

. As long as the partial specific volume of various molecular components remain constant when they are added or substracted from cytoskeleton or solvent, the local net volume growth rate of the total cytoplasm must vanish;

$$R_c(\theta_c, \theta_a) + R_a(\theta_c, \theta_a) \; = 0.$$

Furthermore, since, $\theta_c + \theta_a = 1$ (by definition), we can surmise that $\partial_t(\theta_c + \theta_a) = 0$. Combining this with the two balance equations (25,26), we finally obtain the following mass balance laws for $\theta = \theta_c$ with $f(\theta) := R_c(\theta, 1-\theta)$, namely a

– **hyperbolic transport equation**

$$\partial_t \theta + \nabla \cdot (\theta \; \mathbf{v}) = f(\theta) \; . \tag{27}$$

and the

free divergence for the total volume flux

$$\nabla \cdot (\theta \; \mathbf{v} + (\mathbf{1} - \theta) \; \mathbf{w}) = 0 \; . \tag{28}$$

At any time instant the two velocity fields, $\mathbf{v}$ and $\mathbf{w}$, must jointly satisfy the above divergence condition and also, as the most important constitutional relation for a 'creeping flow' of high viscosity (low Reynolds number), certain pseudo-stationary force balances within an, eventually time dependent, domain $\Omega(t)$ and on its boundary $\partial\Omega(t)$.

2.2 Power Functional and Force Balances for $\Omega(t) = R^m$

Previously we have stated and discussed a system of elliptic differential equations and suitable boundary conditions [14],[15], [17], which describe the pseudostationary **force balances of the two phases** described above. These equations were proposed to hold for creeping flow limit and for isotropic materials. We now show that, for given concentration $\theta = \theta(\mathbf{x}, t)$ at any fixed time t, these equations can also be derived (as Hamilton-Jacobi equations) from minimizing a global functional $J[\mathbf{v}, \mathbf{w}]$ that is a certain measure of the *total work performed per unit time ('power')*:

$$J[\mathbf{v},\mathbf{w}] := \frac{1}{2}\int_\Omega \nabla\mathbf{v}\,\mathbf{M}_c\,\nabla\mathbf{v} + \nabla\mathbf{w}\,\mathbf{M}_a\,\nabla\mathbf{w} + \Phi_c\theta|\mathbf{v}|^2 \tag{29}$$

$$+\frac{1}{2}\int_\Omega \varphi\theta(1-\theta)|\mathbf{v}-\mathbf{w}|^2 \tag{30}$$

$$-\int_\Omega \theta P_c\nabla\cdot\mathbf{v} + (1-\theta)P_a\nabla\cdot\mathbf{w} + P_{ac}(\mathbf{w}-\mathbf{v})\cdot\nabla\theta \tag{31}$$

$$-\int_\Omega \theta\mathbf{F}_c\cdot\mathbf{v} + (1-\theta)\mathbf{F}_a\cdot\mathbf{w} \tag{32}$$

This power functional ought to be minimized in a suitable Sobolev space $\mathfrak{V}$ of all velocity fields $(\mathbf{v},\mathbf{w})$ satisfying the divergence relation (28). The exact formulation is given below.

Before, let us explain the various terms of this functional. The principle is easy and general: Any linear *force balance* vector equation of the form $\Phi(\mathbf{v}) = \mathbf{F}$, where frictional forces equilibrate with inner potential forces or outer field forces, yields, after scalar multiplication by $\mathbf{v}$, a *power balance equation* $\mathbf{D}[\mathbf{v}] = \mathbf{F}\cdot\mathbf{v}$. Here, the *dissipative energy loss rate,* the symmetrical form $\mathbf{D}[\mathbf{v}] := \Phi(\mathbf{v})\cdot\mathbf{v}$, is in balance with the *energy gain rate* due to the effective flow in direction of the applied force field. However, minimizing the *power functional* $J[\mathbf{v}] := \frac{1}{2}\mathbf{D}[\mathbf{v}] - \mathbf{F}\cdot\mathbf{v}$, with the energy gain rate substracted from half the dissipation loss rate, gives back the full force balance vector equation $\Phi(\mathbf{v}_*) = \mathbf{F}$ for the unique minimizer $\mathbf{v}_*$. The minimal 'power' that is attained, $J[\mathbf{v}_*] := \frac{1}{2}\mathbf{D}[\mathbf{v}_*] - \mathbf{F}\cdot\mathbf{v}_* = -\frac{1}{2}\mathbf{D}[\mathbf{v}_*]$, always turns out to be negative.

Analogously, in the power functional above, the two Ω-integrals (29) and (30), which are positive definite, quantify the total rate of dissipation, i.e. conversion of kinematic energy into heat, whereas the following two Ω-integrals (31) and (32) measure the total energy gain rate (or loss rate, if negative) due to the action of internal pressures (P_c , P_a, and P_{ac}) or external forces ($\mathbf{F}_c$ and $\mathbf{F}_a$) on the various phases of the fluid, respectively. More detailed, we now comment the used parameters or parameter functions in the order of their appearance:

- $\mathbf{M}_c = \mathbf{M}_c(\theta)$ and $\mathbf{M}_a = \mathbf{M}_a(\theta)$ denote the viscosities of the complex polymer and aqueous phase, respectively. Both might depend on the volume fraction θ. In particular, we can suppose that $\mathbf{M}_c(\theta) \to 0$ for vanishing polymer concentration $\theta \to 0$. Moreover, notice the tensor notation which, e.g. for $m = 2$, reads $\nabla\mathbf{u}\,\mathbf{M}\,\nabla\mathbf{u} = \mu|\nabla\mathbf{u}|^2 + \lambda(\nabla\cdot\mathbf{u})^2 + \nu(\nabla\times\mathbf{u})^2$.
- The coefficient Φ_c describes a possibly present, distributed body friction (in the 3 dimensional case, for instance induced by a distributed small third phase) or a friction between cytoskeleton and adhesive substrata (important in 2- or 1-dimensional models), see also Section 1.4.1.
- The coefficient φ describes the interphase friction due to the drag between the two velocities with difference vector $(\mathbf{v}-\mathbf{w})$.

The subsequent integral term (31), with the minus sign in front, is the most important term as it describes the volumetric rate of energy supply within the domain Ω. When energy is converted from potential energy material interactions or from molecular motors or from any other processes so as to increase the organized kinematic energy, then these terms are positive. We claim that these simple terms are very general and can include all isotropic constitutive possibilities for supply of mechanical power merely by taking appropriate choices of the three scalar 'static pressures' P_c , P_a, and P_{ac} , as functions of the 'state' θ.

– The first of these (P_c) is a pressure associated purely with the complex polymer phase, e.g. negative if the effect of the microscopic distributed energy supply is to induce an attraction between complex particles (cytoskeletal filaments). If this results in a local contraction of the polymer phase, $\nabla \cdot \mathbf{v} <0$, then the corresponding integrand is positive, meaning that locally kinematic energy is gained. The second (P_a) is an analogous term associated with the aqueous phase. For example, it is positive if aqueous particles tend to separate from each other (e.g. swelling of extracellular matrix). Usually this would induce a local expansion of the aqueous phase, $\nabla \cdot \mathbf{w} >0$, so that the corresponding integrand is again positive, and kinematic is energy is gained locally (e.g. by the use of thermal energy). The third function ($P_{ac} = -P_{ca}$) is a pressure associated with the interface between the two phases. By sign convention the interphase pressure is positive when the two phases tend to avoid each other and negative when they tend to mix with each other. For example, the first case would again describe the process of swelling, in which water could be sucked into the complex polymer phase with a relative velocity 'up-gradient', i.e. $(\mathbf{w} - \mathbf{v}) \cdot \nabla\theta > 0$, leading to kinematic energy gain.

However, the fact that the model interpretations given for the last two pressure integral terms in (31) both rely on the same phenomenon 'swelling', might induce a feeling of redundancy. Indeed, it turns out that the three 'pressures' can be redefined by just adding a joint pressure function

$$P_r(\theta) = \tilde{P}_r(\theta) + \tilde{P}(\theta) \,, \quad r = c, a, ac \tag{33}$$

yielding the additional term $\int \tilde{P}(\theta)\nabla \cdot (\theta\mathbf{v} + (1 - \theta)\mathbf{w}) =0$ in (31). Therefore, because of (31) this redefinition would not change the value of the power functional J . Thus, the solution of the minimization problem does not depend on this redefinition, meaning that a *consistency condition* between the three pressure state functions must hold. For instance, by the particular choice

$$\tilde{P}(\theta) := -\tilde{P}_a(\theta) + \int_0^\theta \frac{\tilde{P}_a(\widetilde{\theta}) + (\widetilde{\theta})\tilde{P}_{ac}}{(1 - \widetilde{\theta})}\, d\widetilde{\theta},$$

we could impose the following differential equation as one possible consistency condition

$$P_a'(\theta) = \frac{1}{1-\theta}(P_a(\theta) + P_{ac}(\theta))$$

implying

$$P_{ac}(\theta)\nabla\theta = \nabla((1-\theta)P_a(\theta)) \tag{34}$$

This equation describes a 'microscopic' force balance, where the aqueous pressure $P_a = P_a(\theta)$ appears to be induced only by an interphase pressure P_{ac} (e.g. hydrophilic swelling forces) such that no other 'intrinsic' pressures in the aqueous phase exist. Notice that (34) implies that the P_r-integrals in (31) after integration by parts (assuming that all terms at $|\mathbf{x}| \to \infty$ vanish) can be simply rewritten as

$$-\int_\Omega \bar{P}(\theta)\nabla\cdot\mathbf{v}$$

yiedling an energy gain/loss term, such as if the *mean intrinsic pressure of the two-phase fluid*

$$\bar{P}(\theta) := \theta P_c(\theta) + (1-\theta)P_a(\theta)\,, \tag{35}$$

would act only on the complex polymer phase flowing with mean velocity $\mathbf{v}$.

Remark 2.14 *A further crucial advantage of this choice of representation for the 'pressure triple' is that the integral on the left hand side is now generally defined for velocities, which are Sobolev functions only, even in occurring cases where the concentration function $\theta = \theta(x,t)$ carries jump discontinuities, so that $\nabla\theta$ would be a measure only, making a definition of the power functional J difficult. Thus, for J to be well defined also for such discontinuous concentrations θ, the condition (33) is required.*

Analogously, we get the following interpretation of the last term in the power functional:

– The integral term (32) describes the supply of mechanical power by body forces ($\mathbf{F}_c$ and $\mathbf{F}_a$) acting on the complex and aqueous phase (this may include gravitational fields, centrifugal fields etc).

From expressions (33) and the argumentation above the question remains, what is the total *pressure acting, for example, in the aqueous phase*? The answer is given by the classical *Lagrange multiplier* technique. Let us assume that $\mathfrak{V}$ is the space of all vector functions $(\mathbf{v},\mathbf{w})$ satisfying (28) such that $\int_\Omega \theta|\nabla\mathbf{v}|^2 + \varepsilon|\nabla\mathbf{w}|^2 < \infty$ and $\int \theta|\mathbf{v}|^2 + \theta(1-\theta)|\mathbf{v}-\mathbf{w}|^2 < \infty$, for given concentration $\theta = \theta(x,t)$. This weighted Sobolev norm is the natural norm making J a coercive functional on $\mathfrak{V}$ (clearly in case of positive body friction Φ_c; otherwise imbedding theorems have to be used).

Then, under suitable conditions on the force fields F, one should be able to proof the following

Proposition 2.15 ***(Definition of pressure p as Lagrange multiplier)*** *For the uniquely determined minimization solution* $(\mathbf{v}_*, \mathbf{w}_*) \in \mathfrak{V}$ *there exists a* unique 'pressure' function p_* *satisfying* $\int \frac{1-\theta}{\theta}|p_*|^2 < \infty$*, such that*

$$DJ[\mathbf{v}_*, \mathbf{w}_*](\mathbf{v}, \mathbf{w}) = -\int_\Omega p_* \nabla \cdot (\theta \mathbf{v} + (1-\theta)\mathbf{w}).$$

We remark that this solution $(\mathbf{v}_*, \mathbf{w}_*, p_*)$ is the unique stationary point of the extended *saddle point type functional*

$$J[\mathbf{v}, \mathbf{w}, p] := \mathbf{J}[\mathbf{v}, \mathbf{w}] - \int_\Omega p \nabla \cdot (\theta \mathbf{v} + (1-\theta)\mathbf{w}).$$

Then, by denoting

$$p_r(x,t) = P_r(\theta(x,t)) + p(x,t)\ , \quad r = c, a, ac$$

the *total pressure* in each phase or at the interphase, respectively, and by writing down the corresponding Hamilton-Jacobi equations, the unique solution $(\mathbf{v}_*, \mathbf{w}_*, p_*)$ of the minimization problem satisfies the following system of elliptic differential equations (written for smooth solutions).

– **Linear elliptic system** for velocities $\mathbf{v}$ and $\mathbf{w}$

$$\nabla \cdot (\mathbf{M}_c \nabla \mathbf{v}) - \nabla(\theta p_c) - p_{ac} \nabla \theta = \varphi \theta (1-\theta)(\mathbf{v} - \mathbf{w}) + \Phi_c \theta \mathbf{v} - \theta \mathbf{F}_c \tag{36}$$

$$\nabla \cdot (\mathbf{M}_a \nabla \mathbf{w}) - \nabla((1-\theta)p_a) + p_{ac} \nabla \theta = -\varphi \theta (1-\theta)(\mathbf{v} - \mathbf{w}) - (1-\theta)\mathbf{F}_a \tag{37}$$

together with the

– **Divergence relation**

$$\nabla \cdot (\theta \mathbf{v} + (1-\theta)\mathbf{w}) = 0\ . \tag{38}$$

Again, here we have used, e.g. for $m = 2$, the following tensor convention $\mathbf{M}\ \nabla \mathbf{u} = \mu \nabla \mathbf{u} + \lambda(\nabla \cdot \mathbf{u})\mathbf{I} + \nu(\nabla \cdot \mathbf{u})\mathbf{I}^\perp$.

These equations together with the **hyperbolic equation** (27) for θ are exactly the classical two-phase flow continuum equations as they were originally derived from a more general modelling setup in [21] by [15], only that the latter authors used quite particular definitions and notations for the pressure terms.

2.3 Vanishing Solvent Viscocity

For further applications let us assume vanishing solvent viscosity $\mathbf{M}_a = 0$, which is reasonable in comparison to the much stronger polymer phase viscosity $\mathbf{M}_a$. Then, under the consistency condition (33) and equation (39) we can derive *Darcy's law for the 'effective pressure'* p, however, only at those points for which $\theta < 1$, that is where still aqueous phase is present:

$$\nabla p = \varphi\theta(\mathbf{v} - \mathbf{w}) - \mathbf{F}_a.$$

Thus the particular choice of the 'pressure triple' reveals the Lagrange multiplier p as a *hydrostatic pressure*, which is mainly related to the draft flow between the tho phases. Thus, we can explicitly express the *solvent velocity* $\mathbf{w}$ in terms of the other variables:

$$\mathbf{w} = \mathbf{v} - \frac{1}{\varphi\theta}\nabla p + \frac{1}{\varphi\theta}\mathbf{F}_a. \tag{41}$$

Finally, summation of eqns. (37) and (39) plus using the divergence relation (40) gives the following

– **Linear Stokes system** for velocity $\mathbf{v}$ and pressure p .

$$\nabla \cdot (\mathbf{M}_c \nabla \mathbf{v}) - \nabla(\bar{P}(\theta) + p) - \Phi\theta\mathbf{v} = \overline{\mathbf{F}} \tag{42}$$

$$\nabla \cdot (\frac{1-\theta}{\varphi\theta}\nabla p - \mathbf{v} + \frac{1-\theta}{\varphi\theta}\mathbf{F}_a) = 0 \tag{43}$$

where the *mean external force* is defined as

$$\overline{\mathbf{F}} := \theta\mathbf{F}_c + (1-\theta)\mathbf{F}_a$$

2.4 Power Functional and Boundary Conditions for Domains $\Omega(t)$ with Piecewise Smooth Boundary

In general, allowing for domains $\Omega(t)$ with boundaries, there will appear boundary integrals in the power functional. Here we restrict to the case that the boundary $\partial\Omega(t)$ can be divided into several parts, a fixed *impermeable boundary* Γ_C, a fixed *permeable boundary* Γ_B, and a *free impermeable boundary* Γ; the first boundary part is assumed to be inert, that is, to carry no extra forces or pressures. (For visualization and application to intracellular polymer dynamics see Fig. 4). Then the *extended power functional* $\widetilde{J}$ has volume integrals as J in (29–32) and, in addition, boundary integrals over Γ and Γ_B, but not over Γ_C:

$$\widetilde{J}[\mathbf{v}, \mathbf{w}] := J[\mathbf{v}, \mathbf{w}]$$

$$+ \int_\Gamma \theta P_c^\Gamma(\mathbf{n}\cdot\mathbf{v}) + (1-\theta)P_a^\Gamma(\mathbf{n}\cdot\mathbf{w}) \tag{44}$$

$$+ \frac{1}{2}\int_{\Gamma_B}(1-\theta)\varphi_B(\mathbf{n}\cdot\mathbf{w})^2 + \int_{\Gamma_B}(1-\theta)P_B(\mathbf{n}\cdot\mathbf{w}). \tag{45}$$

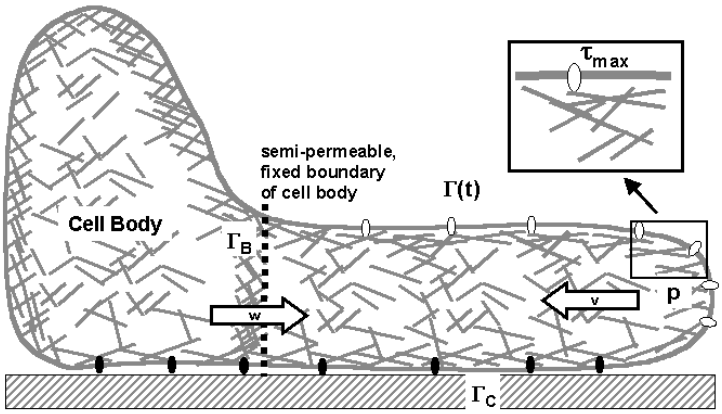

Fig. 6. Sketch of a 2-dimensional cross–sectional model for the two-phase flow dynamics of a cellular pseudopod. It is represented by a time variable domain $\Omega(t)$ with three boundaries: a fixed impermeable boundary Γ_C, where the pseudopod touches a substratum expressing adhesion proteins; another fixed but semi–permeable boundary is Γ_B, where the actin filaments are connected to the stable cytoskeletal cortex of the cell body, while the solvent can pour through with velocity $\mathbf{w}$; finally, a free boundary $\Gamma = \Gamma(t)$ constituting the cortical membrane–protein complex surrounding the pseudopod. The dynamics at the free boundary is determined by a force balance between hydrostatic pressure p and tension τ of the actin filament network that might be pulled inside with inward velocity $\mathbf{v}$, see eq. (58). From [5].

This functional is going to be minimized over all velocity fields $(\mathbf{v}, \mathbf{w}) \in \mathfrak{V}$ defined as in Section 2.2 but now, in addition, satisfying the following conditions at any boundary point of the respective type:

1. At the *fixed impermeable boundary* Γ_C, possibly representing the inert wall of a container in contact with the cell membrane, where the outer normal component of the aqueous flow has to vanish but that of the complex phase flow has to stay non-negative, meaning no outward flow of polymer phase allowed (however, newly assembled polymers near the boundary might flow inward with nonzero velocity as we suppose a 'non sticky' boundary)

$$\mathbf{n} \cdot \mathbf{w} = 0, \ \mathbf{n} \cdot \mathbf{v} \leq 0 \ \ on \ \Gamma_C \tag{46}$$

   with no additional integral term over this part of $\partial\Omega$ appearing in the functional; furthermore
2. At the *fixed permeable boundary* Γ_B, possibly representing the cortical border between a pseudopod and the cell body, where the polymers 'stick'

$$\mathbf{v} = 0 \ \ on \ \Gamma_B \tag{47}$$

   but the aqueous phase is allowed to permeate, thereby experiencing a drag resistance φ_B and an opposing *outer pressure* P_B expressed by the two integral

terms over Γ_B in (45), the first quantifying energy dissipation analogous to the volume dissipation integrand (30), the second analogous to the volume force integrand (32). Finally,

3. at the *free impermeable boundary* $\Gamma = \Gamma(t)$, possibly representing the upper membrane of a pseudopod, which has to move with the total volume flux, i.e.

$$\dot{\Gamma} := \mathbf{n} \cdot (\theta \mathbf{v} + (1-\theta)\mathbf{w}) \tag{48}$$

but again, as on Γ_B, allowing for inward flow of the complex phase, $\mathbf{n} \cdot \mathbf{v} \leq \dot{\Gamma}$, yielding the inequality

$$\mathbf{n} \cdot (\mathbf{v} - \mathbf{w}) \leq 0 \ \ on\ \Gamma \tag{49}$$

Furthermore, there could be a flow resistance due to *outer surface pressures* effecting the complex polymer phase, P_c^Γ, or the aqueous phase, P_a^Γ, at the free boundary. The corresponding integral terms appear in the functional (44).

Now, when deriving the corresponding Hamilton-Jacobi equations, variations by vector functions $\tilde{\mathbf{v}}$, $\tilde{\mathbf{w}} \in \mathfrak{V}$, integration by parts and observation of the imposed boundary conditions (46,47,49) for $\mathbf{v}$ and $\mathbf{w}$, as well as for $\tilde{\mathbf{v}}$ and $\tilde{\mathbf{w}}$, yield the following boundary integrals to appear in the functional derivative

$$\int_{\Gamma_C} (\mathbf{n} \cdot \tilde{\mathbf{v}})(\mathbf{n} \cdot \mathbf{M}_c \nabla \mathbf{v} \cdot \mathbf{n} - \theta p_c) \tag{50}$$

$$\int_{\Gamma_B} (\mathbf{n} \cdot \tilde{\mathbf{w}})(\mathbf{n} \cdot \mathbf{M}_a \nabla \mathbf{w} \cdot \mathbf{n} - (1-\theta)p_a + (1-\theta)(\varphi_B(\mathbf{n} \cdot \mathbf{w}) + P_B)) \tag{51}$$

$$\begin{aligned}\int_{\Gamma} &(\mathbf{n} \cdot \tilde{\mathbf{v}})(\mathbf{n} \cdot \mathbf{M}_c \nabla \mathbf{v} \cdot \mathbf{n} - \theta p_a \theta P_a^\Gamma) \\ &+(\mathbf{n} \cdot \tilde{\mathbf{w}})(\mathbf{n} \cdot \mathbf{M}_a \nabla \mathbf{w} \cdot \mathbf{n} - (1-\theta)p_a + (1-\theta)P_a^\Gamma)\end{aligned} \tag{52}$$

in addition to terms containing the corresponding tangential components of $\mathbf{M}_c$ and $\mathbf{M}_a$, yielding *standard tangential Neumann boundary conditions* for $\mathbf{v}$ and $\mathbf{w}$.

1. Now, at such boundary points of Γ_C where $\mathbf{n} \cdot \mathbf{v} < 0$ holds, $\mathbf{n} \cdot \tilde{\mathbf{v}}$ can be varied arbitrarily with vanishing integral (50), whereas else the integral has only to be nonnegative for all $\mathbf{n} \cdot \tilde{\mathbf{v}} \leq 0$. Thus, we derive the following *Neumann conditions for* $\mathbf{v}$ *on* Γ_C

$$\mathbf{n} \cdot \mathbf{M}_c \nabla \mathbf{v} \cdot \mathbf{n} - \theta p_c \leq 0, \ \text{ and} \tag{53}$$

$$\mathbf{n} \cdot \mathbf{M}_c \nabla \mathbf{v} \cdot \mathbf{n} - \theta p_c \ = 0 \ \text{ for points with } \mathbf{n} \cdot \mathbf{v} < 0 \tag{54}$$

Boundary points in the latter case we characterize by the property *'disrupture'* of the complex phase from the fixed boundary Γ_C, compared to the alternative case *'attachment'*. Notice that these boundary conditions include the effective pressure p because of $p_c = p + P_c(\theta)$.

From such *'disruptive' boundary points* with $\mathbf{n}\cdot\mathbf{v} < 0$, say $y \in \Gamma_C^d$, characteristics x_y for the hyperbolic transport equation (27), i.e. curves satisfying $\dot{x}_y(t) = \mathbf{v}\,(t, x_y(t))$ and $x_y(t_0) = y$, emanate into the domain $\Omega(t)$, so that we need an additional condition which (for applications) is chosen as a homogeneous

Dirichlet boundary condition for the *hyperbolic equation*:

$$\theta(t,y) = 0 \text{ for } y \in \Gamma_C^d(t)\,. \tag{55}$$

The expression $\tau_c := \mathbf{n}\cdot\mathbf{M}_c\nabla\mathbf{v}\cdot\mathbf{n} - \theta p_c$ appearing in (53,54), can be regarded as the *tension (or stress) within the complex polymer phase*. This polymer stress at the fixed boundary could become negative in the case of attachment (e.g. during expansive swelling) but never positive (i.e. contractile), because then disrupture of polymers would occur, whence the stress becomes zero. Indeed, this condition is consistent with (54) since in case of disrupture the polymer concentration θ at the boundary vanishes (55) and with it the viscosity tensor $M_c(\theta)$.

2. Since variations of $\mathbf{n}\cdot\tilde{\mathbf{w}}$ in (51) are free on the permeable part of the fixed boundary, we conclude the following *generalized Neumann conditions for* $\mathbf{w}$ *on* Γ_B

$$\mathbf{n}\cdot\mathbf{M}_a\nabla\mathbf{w}\cdot\mathbf{n}/(1-\theta) + \varphi_B(\mathbf{n}\cdot\mathbf{w}) = p + P_a(\theta) - P_B \tag{56}$$

or, in the limiting case of relatively small aqueous viscosity $\mathbf{M}_a$ and cortical boundary flow resistance φ_B, just the simple *Dirichlet condition for* p on Γ_B

$$p = P_B - P_a(\theta). \tag{57}$$

3. Finally, on the free boundary Γ we first perform variations in $\tilde{\mathbf{v}}$ and $\tilde{\mathbf{w}}$ satisfying the equality $\mathbf{n}\cdot(\tilde{\mathbf{v}} - \tilde{\mathbf{w}}) = 0$ and obtain the following *Neumann condition* for $\mathbf{v}$ and $\mathbf{w}$ on Γ

$$\mathbf{n}\cdot\mathbf{M}_c\nabla\mathbf{v}\cdot\mathbf{n} + \mathbf{n}\cdot\mathbf{M}_a\nabla\mathbf{w}\cdot\mathbf{n} = p + \theta(P_c(\theta) - P_c^\Gamma) + (1-\theta)(P_a(\theta) - P_a^\Gamma). \tag{58}$$

In addition, variations satisfying $\tilde{\mathbf{w}} = -\tilde{\mathbf{v}}$ and, in case of a boundary point with $\mathbf{n}\cdot(\mathbf{v}-\mathbf{w}) = 0$ also $n\cdot(\tilde{v} - \tilde{w}) \le 0$, induce the additional properties

$$\mathbf{n}\cdot\mathbf{M}_a(\nabla\mathbf{w})\cdot\mathbf{n}/(1-\theta) \ge p + P_a(\theta) - P_a^\Gamma \text{ and} \tag{59}$$

$$\mathbf{n}\cdot\mathbf{M}_a(\nabla\mathbf{w})\cdot\mathbf{n}/(1-\theta) = p + P_a(\theta) - P_a^\Gamma \text{ if } \mathbf{n}\cdot(\mathbf{v}-\mathbf{w}) < 0. \tag{60}$$

In the vanishing viscosity case $\mathbf{M}_a = 0$, assumed in the previous Section 2.3, these turn out to be *Dirichlet conditions for* p on Γ_B

$$p \le P_a^\Gamma - P_a(\theta) \quad \text{and} \tag{61}$$

$$p = P_a^\Gamma - P_a(\theta) \quad \text{for } \mathbf{n}\cdot(\mathbf{v}-\mathbf{w}) < 0. \tag{62}$$

Thus, in this case we obtain the following

Derived model system describing a *strongly viscous two-phase polymer flow with relatively low aqueous viscosity:* For each minimal solution of the power functional $\widetilde{J}[\mathbf{v}, \mathbf{w}]$ defined at the beginning of this Section, in the limit $\mathrm{M}_a = 0$, we have derived, at least in a weak sense, the equations (27) and (42,43) as well as the derived boundary conditions above, that is a

– **hyperbolic-elliptic system of generalized Stokes type** on $\Omega(t)$

$$\partial_t \theta + \nabla \cdot (\theta\, \mathbf{v}) = f(\theta) \tag{63}$$

$$\nabla \cdot (\mathbf{M}_c(\theta)\nabla \mathbf{v}) - \nabla(\bar{P}(\theta) + p) - \Phi_c \theta \mathbf{v} = \overline{\mathbf{F}} \tag{64}$$

$$\tag{65}$$

$$\nabla \cdot (\frac{1-\theta}{\varphi\theta}\nabla p - \mathbf{v} + \frac{1-\theta}{\varphi\theta}\mathbf{F}_a) = 0 \tag{66}$$

with **boundary conditions** for velocity $\mathbf{v}$ and pressure p, being inequalities or equalities on different parts of the boundary $\partial\Omega(t)$, namely in addition to 'natural' *tangential boundary conditions* mentioned above, the Neumann conditions (53,54) for $\mathbf{v}$ on the fixed impermeable boundary Γ_C with hyperbolic 'Dirichlet' condition (55) for θ, the Dirichlet condition (57) for p on the fixed impermeable boundary Γ_B as well as the Dirichlet conditions (61,62) for p and the Neumann condition (58) for $\mathbf{v}$ on the free impermeable boundary Γ. The normal speed $\dot{\Gamma}$ of the free boundary is explicitly given by equation (48) with $\mathbf{w}$ substituted as in (41).

2.5 Applications to Cytoplasm Flow and 1-Dimensional Examples

These derived two-phase flow equations of generalized Stokes type have been applied to several biological problems of cell motility, whereby particularly the two pressure terms $P_c(\theta)$ and $P_a(\theta)$ had to be chosen appropriately, for further discussions we refer to [17] and [5]. For example, the following results have been obtained: 3-dimensional rotationally symmetric model simulations for cell division, with detailed reproduction of experimental data for *Xenopus* eggs [23], 3-dimensional model for cytoplasm streaming in *Amoeba proteus* [18], 2-dimensional simulations of local cytoplasm protrusions [16], 2-dimensional movement of *Listeria* bacteria in the cytoplasm [26] and, as application in the simple 1-dimensional case, model simulations for lamellipodial protrusions and retractions [3],[5]. Here the domain $\Omega(t)$ is a finite interval with fixed (permeable) boundary point on one side (towards the cell body) and free (impermeable) boundary at the other side (the lamellipodial tip). In order to reproduce corresponding experimental observations from motility of human epidermal cells [2], the conditions for attachment and disrupture had to be slightly generalized by including stress dependent release of polymer binding to surface molecules; for more details and numerical simulations see [5].

However, already on fixed domains further simulations of the 1-dimensional hyperbolic-elliptic Stokes system reveal interesting dynamical properties of these

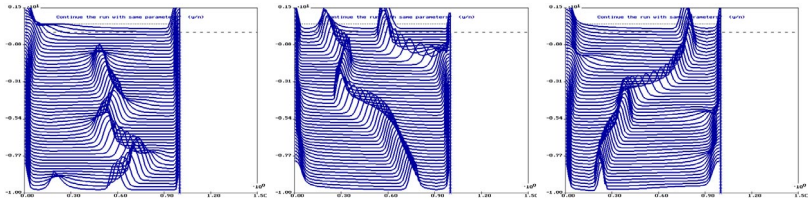

Fig. 7. 1-dimensional model simulation of a contractile, reactive and highly viscous two-phase fluid showing chaotic wave dynamics. Plot of actin polymer density $\theta(t, x)$ over a fixed spatial interval (horizontal) and over time in three successive panels (time running from 0 to 45 min, vertically from top to bottom in each panel)

viscous two-phase polymer flows. Indeed, for parameter choices such that the trivial constant state is dynamically unstable and dissipative friction is large enough, there appear solutions which are of chaotic character in time. For periodic boundary conditions in space (say a 1-dimensional polymer ring, e.g. actin filaments around a cell spread on a 2-dimensional substratum) they had been observed already by [14], where a standing wave showed (though very slight) irregular oscillations in amplitude and position. Moreover, simulations with fixed 'sticky' boundaries, i.e. zero flow conditions on both sides, have shown ongoing chaotic waves appearing in the interior, oscillating in position until finally they drift to one of the boundaries and melt there with persistent boundary layers, see Fig. 6 in [5] as well as Fig. 7.

2.6 Discussion

The appearance of such chaotic dynamics in the two-phase flow system strongly depends on the fact, that the constitutive law for the 'mean pressure' $\bar{P}(\theta) := \theta P_c(\theta) + (1-\theta)P_a(\theta)$ (35) in Stokes equation (42) for the velocity provides a **cubic non-linearity** which distinguishes regions of low polymer concentration θ with 'swelling' properties from regions of medium concentration θ having 'contractile' properties, i.e. where $\bar{P}'(\theta) < 0$. Thus, with such types of non-linearities, the polymer flow equations above model a **contractile and reactive, highly viscous two-phase fluid**.

Therefore it becomes clearly evident, why the chaotic wave phenomena in these 'deterministic fluids' have such different features when compared to the very constant speed waves appearing in the 'stochastic bird swarm fluids' of Chapter 1: There the derived continuum (Navier-Stokes) equations have a **monotone** 'attraction-repulsion function' as constitutive law for the 'elastic tension' $\alpha(u)$ in the infinitesimal network of (nearest) neighbors, see (22), and the globally stable constant equilibrium state has to be fed by continuing noise to produce such waves.

For the minimization problem presented in this Chapter 2, there remain several challenging difficulties to overcome in order to prove theorems on unique existence. One difficulty concerns the choice of suitably weighted Sobolev spaces $\mathfrak{V}$ in domains with boundaries, particularly in situations where the polymer concentration

degenerates, $\theta \to 0$, at boundary points, as it occurs in cases of 'disrupture' (see Section 2.4). Even for proofs in the 1-dimensional case one probably needs uniform estimates of θ from below like $\theta(t,x) \succeq dist_{\partial\Omega}(x)$.

Furthermore, spatial discretizations of the elliptic Stokes system (say in week form) have to regard the fact that the leading (elliptic) coefficient in the velocity equation (65) degenerates to zero, for $\theta \to 0$, whereas that in the pressure equation (66) degenerates to infinity. Suitable discretization procedures at the boundaries, similar to those that have been used in 1-d [5], should be able to master this problem. However, with regard to the second equation it is essential for this class of solution procedures to guarantee a uniform bound $\theta \leq \theta_{\max} < 1$. Violation leads to a singular perturbed problem: For $\theta \to 1$ the hyperbolic two-phase flow system above degenerates into the incompressible stationary Stokes equations. Indeed, under the assumption $f(1) = 0$, i.e. if no polymer assembly or disassembly take place in the saturated domain $\Omega_1(t) := \{x \in \Omega(t) | \theta(t,x) = 1\}$, then there both equations, the hyperbolic (64) and the elliptic (66), change their type and merge into the simple incompressibility condition $\nabla \cdot \mathbf{v} = 0$. Recently, our Egyptian doctor student Mahmoud Mansour [29] could prove (by local singularity analysis and by using two different numerical simulation techniques) the existence of travelling front solutions $0 < \theta(x - ct) \leq 1$ for these 1-dimensional degenerate equations, with a uniquely determined minimal travelling speed c_* corresponding to the well-known minimal Fisher's diffusion speed; in fact, supposing a suitable behavior of the viscosity term $|\mathbf{M}_c(\theta)| \sim \theta^2$, for $\theta \to 0$ the hyperbolic two-phase flow system converges to a diffusion equation.

The last mentioned result is not only applicable to polymer dynamics, but also to the dynamics of interactively moving cells in the process of tissue formation (particularly for simulating wound healing). In contrast to the stochastic multi-particle approach pursued in Chapter 1, here – by assuming an already performed homogenization process – the more or less connected cells (eventually including extracellular matrix filaments connecting them) are modelled as the *complex phase*, whereas the surrounding *aqueous medium* is modelled as the other phase. Indeed, as a further generalization of the presented model class of two-phase flows, Sharon Lubkin [27] used a three-phase model to simulate the dynamical development of embryonal lung tissues, where two types of cells and the intercellular medium play their role. Moreover, I would like to emphasize and stimulate potential ideas to generalize the Voronoi-Delaunay concepts in order to derive such 'multi-phase' continuum equations for polymer networks and cell tissues directly from suitable interactive stochastic 'multi-particle' processes.

Thus, by taking a synopsis of Chapters 1 and 2 and realizing the various modelling derivations and simulation techniques that can lead to hyperbolic continuum equations of generalized Navier-Stokes type, we might express an increasing confidence towards a successful mathematical treatment of the rich spectrum of current and future complex problems offered by interdisciplinary research on interactive motion in biological systems.

Acknowledgements. The presented thoughts and formulations are the synergetic result of (since more than 15 years) ongoing scientific exchange between working groups in the Division of Theoretical Biology and the Institute of Applied Mathematics at the University of Bonn, mainly within the DFG special research program on 'Nonlinear Partial Differential Equations' (SFB 256). For Chapter 1 my particular thanks go to Martin Grothaus, Juri Kondratjev and Serge Albeverio for discussing the stochastic aspects of continuum limits, as well as to Hans-Wilhelm Alt for jointly looking at various analytic aspects, also for Chapter 2. The implementation of Voronoi-Delaunay methods into modelling of bird swarms and corresponding 2-dimensional simulations (including an extended statistical analysis) have been carefully and gratefully performed by Ralf Müller within his diploma theses. Chapter 2 essentially is a revision of a hitherto unpublished manuscript jointly written, over a longer time of fruitful collaboration and visit exchanges, with Micah Dembo in the Department of Biomedical Engineering at Boston University; special thanks to him for joint authorship with the bunches of good ideas and critical remarks.

Several authors of important work and publications related to both Chapters and partially mentioned in the list of references, who have been of grateful influence upon shaping my own modelling concepts, were active participants in a series of SFB-Workshops which I could organize together with colleagues and friends from the worldwide Mathematical Biology and Applied Mathematics community. There was the early Workshop in 1989 on 'Biological Motion' with Leah Edelstein-Keshet, Andreas Huth, Bob Tranquillo, beside others [1], a subsequent Workshop in 1995 on 'Cell and Tissue Motion' with Micah Dembo, Hans G. Othmer, Rich Dickinson [4] and a recent Workshop on 'Polymer and Cell Dynamics' again with Micah Dembo, then with Michael Griebel, Mark Chaplain, Dirk Drasdo, Eirikur Palsson and others [8]; to all of them my thankful acknowledgment as well as to Anke Thiedemann for being the effective and nice soul of the whole organization. Finally and most closely, I want to thank all the younger collaborators and students in our Theoretical Biology group but also my colleagues from mathematics and biosciences in Bonn, who helped to built and develop the lively mental and social nest that became the essential base for my own scientific work on modelling, simulation and analysis in biology; among these and in connection with the presented topic, I would particularly like to mention Jürgen Lenz, Beate Pfistner, Thomas Pohl, Guido Scholz, Volker Lendowski, Edith Geigant, Andreas Deutsch, Michael Wurzel, Ralf Müller, Arne Rüter, Dieter Felix, Boris Hinz, Till Bretschneider, Thorsten Libotte, Ulrike Schuldenzucker, Claudia Mulder and Mahmoud Mansour.

References

1. W. Alt, G. Hoffmann (eds.) (1990): Biological Motion. Lecture Notes in Biomath. vol. 89, Springer-Verlag, Berlin
2. W. Alt, O. Brosteanu, B. Hinz and H.W. Kaiser (1995): Patterns of spontaneous motility in videomicrographs of human epidermal keratinocytes (HEK). Biochemistry and Cell Biology, **73**, 441–459

3. W. Alt (1996): Biomechanics of actymyosin mediated motility of keratinocytes. Biophysics, **41**, 181–188
4. W. Alt, A. Deutsch, G. Dunn (eds.) (1997): Dynamics of Cell and Tissue Motion. Birkhäuser-Verlag, Basel, Boston, Berlin
5. W. Alt, M. Dembo (1999): Cytoplasm dynamics and cell motion: two-phase flow models. Math. Biosciences, **156**, 207–228
6. W. Alt (2002): One-dimensional dynamics of stochastic skeins: condensation waves and continuum limits. Submitted to J. Math. Biol.
7. W. Alt, T. Bretschneider, R. Müller (2002): Interactive movement, aggregation and swarm dynamics. In: W.Alt, M.Chaplain, M.Griebel, J.Lenz (eds.) Polymer and Cell Dynamics – Multiscale Modelling and Numerical Simulation. To appear in Birkhäuser-Verlag, Basel
8. W. Alt, M. Chaplain, M. Griebel, J. Lenz (eds.) (2002): Polymer and Cell Dynamics – Multiscale Modelling and Numerical Simulation. To appear in Birkhäuser-Verlag, Basel
9. D.C. Bottino (1998): Modeling viscoelastic networks and cell deformation in the context of the immersed boundary method. J. Comp. Phys., **147**, 86–113
10. D.C. Bottino (2001): Computer simulations of mechanochemical coupling in a deforming domain: Applications to cell motion. Preprint
11. T. Bretschneider (2002): Reinforcement of cytoskeleton-matrix bounds and tensiotaxis: a cell based model. In: A.Deutsch et al. (eds) Function and Regulation of Cellular Systems: Experiments and Models. To appear in Birkhäuser-Verlag, Basel
12. Z. Csahok, A. Czirok (1997): Hydrodynamics of bacterial motion. Physica A, **243**, 304–318
13. A. Czirok, T. Vicsek (2000): Collective behaviour of interacting self-propelled particles. J. Phys. A, **281,**17–29
14. M. Dembo, F.W. Harlow, W. Alt (1984): The biophysics of cell surface mobility. In: (A.D.Perelson, Ch.DelLisi, F.W.Wiegel eds.) *Cell Surface Dynamics, Concepts and Models*. Marcel Dekker, New York, Basel, 495–542
15. M. Dembo, F.W. Harlow (1986): Cell motion, contractile networks, and the physics of interpenetrating reactive flow. Biophys. J., **50**, 109–121
16. M. Dembo (1986): The mechanics of motility in dissociated cytoplasm. Biophys. J., **50**, 1165–1183
17. M. Dembo (1989): Field theories of the cytoplasm. Comments theor. Biol., **1**, 159
18. M. Dembo (1994): On free boundary problems and amoeboid motion. In: N. Akkas (ed) Biomechanics of Active Movement and Division of Cells. NATO ASI Ser. H84. Springer, Berlin, p. 231
19. M. Dembo, Y. Wang (1999): Stresses at the cell-to-substrate interface during locomotion of fibroblasts. Biophys. J., **76**, 2307–2316
20. D. Drasdo (2002): On selected individual-based approaches to the dynamics in multicellular systems. In: W.Alt, M.Chaplain, M.Griebel, J.Lenz (eds) Polymer and Cell Dynamics – Multiscale Modelling and Numerical Simulation. To appear in Birkhäuser-Verlag, Basel
21. D.A. Drew, L.A. Segel (1991): Averaged equations for two phase flow. Stud. Appl. Math., **50**, 205–231
22. W. Ebeling, F. Schweitzer (2001): Swarms of particle agents with harmonic interactions. Theory in Biosciences, **120**, 207–224
23. X. He, M. Dembo (1997): On the mechanics of the first cleavage division of the sea urchin egg. Exper. Cell Res., pp. 233–252

24. F.H. Heppner, U. Grenander (1990): A stochastic nonlinear model for coordinated bird flocks . In: S. Krasner (ed) The Ubiquity of Chaos. Washington, DC: American Association for the Advancement of Science.
25. H. Holden, B. Oksendal, J. Uboe, T. Zhang (1996): Stochastic Partial Differential Equations. A modeling white noise functional approach, Birkhäuser, Basel
26. V. Lendowski, A. Mogilner (1997): Origin of actin-induced locomotion of *Listeria*. In: W.Alt, A.Deutsch, G.Dunn (eds) Dynamics of Cell and Tissue Motion. Birkhäuser-Verlag, Basel, Boston, Berlin, 93–99
27. S. R. Lubkin, T. Jackson (2001): Multiphase Mechanics of Capsule Formation in Tumors. J. Biomech Eng, in press
28. T. Oliver, M. Dembo, K. Jacobson (1999): Seperation of propulsive and adhesive traction stresses in locomoting keratocytes. J. Cell Biology, **145**, 589–604
29. M. Mansour (2001): Singularity analysis of travelling wave solutions for degenerate diffusion and transport equations modelling cell motility. PhD thesis, Univ. Bonn
30. F.A. Meinicke, S.C. Potten, M. Loeffler (2001): Cell migration and organization in the intestinal crypt using a lattice-free model. Cell Prolif., **34**, 253–266
31. R. Müller (2002): Dynamik in stochastischen Vielteilchensystemen zur Modellierung von Vogelschwärmen. Diploma thesis Univ. Bonn
32. K. Oehlschläger (1989): On the derivation of reaction-diffusion equations as limit dynamics of systems of moderately interacting stochastic processes. Th. Rel. Fields, **82**, 565–589
33. K. Oehlschläger (1991) On the connection between Hamiltonian many-particle systems and the hydrodynamical equations. Arch. Rat. Mech. Anal., **115**, 297–310
34. S. Olla, S.R.S. Varadhan, H.T. Yau (1993): Hydrodynamical limit for a Hamiltonian system with weak noise. Comm. Math. Phys., **155**, 523–560
35. J. Toner, Y. Tu (1995): How birds fly together: Long range oder in a two-dimensional dynamical XY model. Phys. Rev. Lett. **75**, 4326–4329
36. J. Toner, Y. Tu (1998): Flocks, herds and schools: A quantitative theory of flocking. Phys. Rev. E, **58**, 4828–4858